action of morphine and on the associative processes involved in the development of tolerance and dependence.

Our results suggest a potentially important role for NMDA receptors in the development of opiate tolerance and dependence. MK-801 also interferes with the development of sensitization (or reverse tolerance) to stimulant drugs (*12*), suggesting that excitatory amino acid systems may be involved in experience-dependent changes produced by repeated exposure to a variety of drugs. Adjunctive treatment with drugs that interfere with tolerance and dependence may prove valuable for extending the usefulness of opiates clinically.

REFERENCES AND NOTES

1. D. H. Clouet and K. Iwatsubo, *Annu. Rev. Pharmacol.* **15**, 49 (1975); H. O. J. Collier, *Nature* **283**, 625 (1980); C. W. Sharp, Ed., *NIDA Res. Monogr. 54* (1984); S. M. Johnson and W. W. Fleming, *Pharmacol. Rev.* **41**, 435 (1989).
2. G. K. Aghajanian, *Nature* **276**, 186 (1978); R. Andrade *et al.*, *Eur. J. Pharmacol.* **91**, 161 (1983); R. A. North *et al.*, *Proc. Natl. Acad. Sci. U.S.A.* **84**, 5487 (1987); M. J. Christie, J. T. Williams, R. A. North, *Mol. Pharmacol.* **32**, 633 (1987); M. J. Christie, J. T. Williams, R. A. North, *NIDA Res. Monogr.* **78**, 158 (1987).
3. A. Wikler, *Am. J. Psychiatry* **105**, 329 (1948); *Arch. Gen. Psychiatry* **28**, 611 (1973); *Pavlovian J. Biol. Sci.* **11**, 190 (1976); S. Siegel, *Science* **193**, 323 (1976).
4. S. Siegel, in *Research Advances in Alcohol and Drug Problems*, Y. Israel, F. B. Glaser, H. Kalant, R. E. Popham, Eds. (Plenum, New York, 1983), p. 207; T. B. Baker and S. T. Tiffany, *Psychol. Rev.* **92**, 78 (1985); A. J. Goudie and C. Demellweek, in *Behavioral Analysis of Drug Dependence*, S. R. Goldberg and I. P. Stolerman, Eds. (Academic Press, Orlando, FL, 1986), p. 225; B. A. Ray, Ed., *NIDA Res. Monogr. 84* (1988).
5. C. W. Cotman and L. L. Iversen, *Trends Neurosci.* 7, 263 (1987); G. L. Collingridge and R. A. J. Lester, *Pharmacol. Rev.* **40**, 143 (1989); J. C. Watkins and G. L. Collingridge, Eds., *The NMDA Receptor* (Oxford Univ. Press, New York, 1989).
6. Adult male Sprague-Dawley rats were used in all experiments. In acute studies, animals received an intraperitoneal (ip) injection of saline (1 ml/kg) or MK-801 followed 30 min later by a subcutaneous (sc) injection of saline or morphine sulfate. The analgesic response to morphine was assessed by the tail-flick test (7) 60 min after the second injection. For chronic studies, animals received injections twice daily (8:00 and 17:00) for 9 days. On odd-numbered days, analgesic response was assessed by the tail-flick test 60 min after the morning morphine injection. In experiment 1, treatment groups included (pretreatment:treatment) (i) saline:saline; (ii) saline:10 mg/kg morphine; (iii) 0.1 mg/kg MK-801:saline; and (iv) 0.1 mg/kg MK-801:10 mg/kg morphine. Control experiments were performed on day 10 in the same group of animals to determine whether MK-801 affected the development of tolerance or whether it simply altered the behavioral expression of the analgesic response. On this day treatments were reversed so that animals that had been treated with MK-801 followed by morphine on days 1 through 9 were challenged with saline followed by morphine, and animals that had been treated with saline followed by morphine on days 1 through 9 were challenged with MK-801 followed by morphine. In addition, animals that had received chronic treatment with MK-801 followed by saline were challenged with MK-801 followed by morphine. Immediately after the tail-flick test on day 10, animals were injected with naloxone (2 mg/kg sc) to precipitate withdrawal. The withdrawal syndrome was assessed by placing each rat in a 45-cm-high plexiglass box and recording the incidence of escape jumps (*8*) for 15 min. In experiment 2 the dose-dependent effects of MK-801 were examined. On days 1 through 9, animals were treated with saline or MK-801 (0.03, 0.1, or 0.3 mg/kg ip) followed 30 min later by morphine (10 mg/kg sc). Tail-flick latencies were determined on odd-numbered days, as described above. In this experiment, animals received no pretreatment on day 10, but received a morphine challenge, followed by the tail-flick test and naloxone-precipitated withdrawal 60 min after the morphine injection.
7. F. E. D'Amour and D. L. Smith, *J. Pharmacol. Exp. Ther.* 72, 74 (1941). Two to three successive determinations were made for each rat, and the mean of these scores was used as the tail-flick latency for that animal. A 10-s cutoff was used to minimize tissue damage from the heat lamp.
8. D. L. Francis and C. Schneider, *Br. J. Pharmacol.* **41**, 424P (1971); E. Wei, *Psychopharmacology* **28**, 35 (1973); J. Bläsig *et al.*, *ibid.* **33**, 19 (1973).
9. We do not believe that our results were due to motor impairment of the animals. The tail-flick response is a specific indicator of opiate analgesia in rats and is very resistant to nonspecific impairment [J. W. Lewis, G. Baldrighi, H. Akil, *Brain Res.* **424**, 65 (1987)]. In addition, control experiments on day 10 suggest that motor impairment was not responsible for the observed effects. Our results cannot be explained by altered morphine metabolism produced by MK-801 since there was no increase in withdrawal signs in MK-801–treated animals as would be expected if morphine concentrations were increased during the course of treatment. Finally, it is unlikely that the effects were due to MK-801–dependent hypothermia [A. Buchan and W. A. Pulsinelli, *J. Neurosci.* **10**, 311 (1990)] since MK-801 does not, by itself, produce a decrease in body temperature [D. G. Nehls *et al.*, *Brain Res.* **511**, 271 (1990)].
10. Electrophysiological studies on single locus ceruleus neurons have suggested that excitatory amino acids may be involved in opiate withdrawal. [K. Rasmussen and G. K. Aghajanian, *Brain Res.* **505**, 346 (1989); C.-S. Tung, J. Greenhoff, T. H. Svensson, *Acta Physiol. Scand.* **138**, 581 (1990)].
11. There are two distinct types of drug tolerance: associative tolerance and nonassociative tolerance. Nonassociative tolerance is produced by high doses of opiates and is not affected by environmental or behavioral manipulation of the animal. Associative tolerance is very sensitive to behavioral and pharmacological manipulations that modulate learning and memory, and in fact may result primarily from learning processes such as classical conditioning, instrumental conditioning, or habituation [(*4*); S. T. Tiffany and P. M. Maude-Griffen, *Behav. Neurosci.* **102**, 534 (1988); R. Dafters and J. Odber, *ibid.* **103**, 1082 (1989)]. The present experiments did not distinguish between associative and nonassociative tolerance.
12. R. Karler *et al.*, *Life Sci.* **45**, 599 (1989); H. E. Criswell *et al.*, *Brain Res.* **512**, 284 (1990).
13. L. S. Harris and A. K. Pierson, *J. Pharmacol. Exp. Ther.* **143**, 141 (1964).
14. The highest dose of MK-801 (0.3 mg/kg) in combination with 10 mg/kg morphine proved to be toxic to the animals—three animals died on the first day of treatment and others appeared sick and lost weight over the days of treatment. Because of this toxicity, the 0.3 mg/kg dose of MK-801 was discontinued after the morning of day 5, and the three remaining animals in the group were pretreated with saline for the remainder of the experiment. Despite the discontinuation of MK-801 treatment, these animals showed nearly complete inhibition of morphine tolerance, remaining strongly analgesic to morphine throughout the study (after the discontinuation of morphine pretreatment these animals rapidly regained their health). Animals receiving 0.03 and 0.1 mg/kg of MK-801 in combination with 10 mg/kg of morphine appeared quite healthy throughout treatment, and had no untoward weight loss.

15. We thank S. Watson, D. Bronstein, J. Herman, and T. Robinson for helpful comments on the manuscript and L. Fox and J. Olds for encouragement and inspiration. Supported by National Institute on Drug Abuse (NIDA) National Research Service Award DA05336 to K.A.T., NIDA grant DA02265, National Institute of Mental Health grant MH422251, the T. Raphael Research Fund, and the Lucille B. Markey Charitable Fund to H.A.

23 July 1990; accepted 19 October 1990

Critical Structural Elements of the VP16 Transcriptional Activation Domain

W. DOUGLAS CRESS AND STEVEN J. TRIEZENBERG*

Virion protein 16 (VP16) of herpes simplex virus type 1 contains an acidic transcriptional activation domain. Missense mutations within this domain have provided insights into the structural elements critical for its function. Net negative charge contributed to, but was not sufficient for, transcriptional activation by VP16. A putative amphipathic alpha helix did not appear to be an important structural component of the activation domain. A phenylalanine residue at position 442 was exquisitely sensitive to mutation. Transcriptional activators of several classes contain hydrophobic amino acids arranged in patterns resembling that of VP16. Therefore, the mechanism of transcriptional activation by VP16 and other proteins may involve both ionic and specific hydrophobic interactions with target molecules.

VP16 (ALSO TERMED V_{mw65} OR α-TIF) is a protein component of the herpes simplex virus type 1 (HSV-1) virion that specifically and potently activates transcription of the viral immediate-early (IE) genes (*1*). Molecular genetic studies of VP16 have distinguished two functional domains that are relevant to transcriptional activation. The specificity for IE genes is conferred by the interaction of an NH_2-terminal portion of VP16 with host proteins that bind IE cis-regulatory elements (*2*). The

Department of Biochemistry, Michigan State University, East Lansing, MI 48824–1319.

*To whom correspondence should be addressed.

transcriptional activation domain in the COOH-terminal 78 amino acids of VP16 (*3, 4*) activates transcription when attached to a heterologous DNA-binding domain and is an unusually strong activator (*5, 6*).

The preponderance of acidic amino acids within various transcriptional activation domains (*7*), including that of VP16, suggests that negative charge is a critical component of the activation domain structure. We tested whether activation by VP16 is related simply to the net negative charge by replacing, in various combinations, the acidic amino acids within the activation domain with uncharged residues. The minimal VP16 activation domain targeted for mutagenesis (VP16 codons 427 to 451) includes ten acidic amino acid residues (Fig. 1). This minimal activation domain retains about one-half of the activity of the full-length domain (*3*).

The ability of each VP16 derivative to activate IE gene transcription was measured by a transient transfection assay (*3*) in which a plasmid that expressed the wild-type or a mutant VP16 protein was cotransfected with both an indicator plasmid and an internal control plasmid. From the relative activities of 21 such mutants (Fig. 2), we infer that negative charge is an important feature of the VP16 activation domain. Replacement of increasing numbers of acidic residues with uncharged residues led to a progressive decrease in transcriptional activation. Removal of seven or more negative charges inactivated the protein beyond our level of detection. However, net negative charge was not the sole determinant of activity, because some derivatives with identical net negative charge had distinguishable activities. For instance, DN2 was less active than DN6; DN1234 was less active than DN5678; DN1-4,910 was less active than DN5-10; and DN123,5-8 was less active than DN4-10. In each of these cases, mutations of negative residues 1, 2, and 3 had a greater effect on activity than mutations at the other positions, suggesting that charge distribution, secondary structure, or both also contribute to activity.

Acidic activation domains have been modeled as amphipathic α helices (AAHs) (*8*). Indeed, secondary structure predictions for the VP16 amino acid sequence suggested that its activation domain could form an AAH (*6*). We tested the role of predicted amphipathy by constructing a series of VP16 derivatives from which we removed blocks of four negatively charged residues circularly permuted about the putative AAH. We reasoned that activation domains altered in the center of the charged face of the putative AAH would likely be strongly affected in transcriptional activation, whereas mutations affecting the periphery of the charged face might be only slightly affected. However, the relative activities of these VP16 derivatives showed no correlation between transcriptional activation and predicted amphipathy (Fig. 3). For instance, the mutants DN34610 and DN34510 each lack acidic residues in the center of the charged face of the putative AAH, yet their activities were higher than those of mutants DN1789 and DN2789, which retain negative charges on the putative charged surface.

Because we observed no relation between predicted amphipathy and transcriptional activation, we tested whether the function of VP16 depended on the predicted α helicity. The cyclic side chain of proline cannot be accommodated into an α helix. Therefore, we replaced selected amino acids with proline residues to disrupt the predicted α helical structure in three regions across the activation domain. This series included two constructs with single substitutions at His^{425} (HP425) or Phe^{442} (FP442), and one with substitutions at both Ala^{432} and Ala^{436} (AP432/6). This double mutation was constructed because this region possessed the greatest predicted helix-forming tendencies. Neither HP425 nor AP432/6 had a detectable effect on activation by VP16 (Fig. 4A), suggesting that the predicted helical structure is not critical for activation. However, the proline substitution at Phe^{442} abolished transcriptional activation by VP16. This substitution apparently did

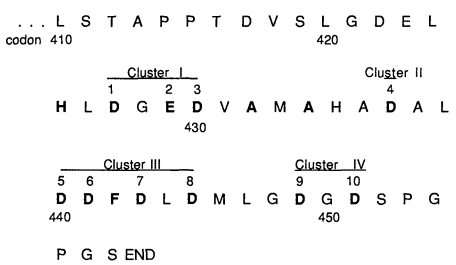

Fig. 1. Amino acid sequence of the minimal activation domain of VP16 (*16*). The amino acids targeted for mutagenesis are indicated by bold letters; the acidic residues are numbered 1 to 10. The codons for the ten acidic amino acids were mutagenized (*17*) in four clusters with the use of mixed-sequence oligonucleotides to generate all combinations of desired substitutions within each cluster. Activation domain derivatives with as many as ten mutations were then constructed by making intercluster recombinants with convenient restriction sites. Altered activation domain DNA fragments were substituted into the parental VP16 expression plasmid, pMSVP16 del456 (*3*).

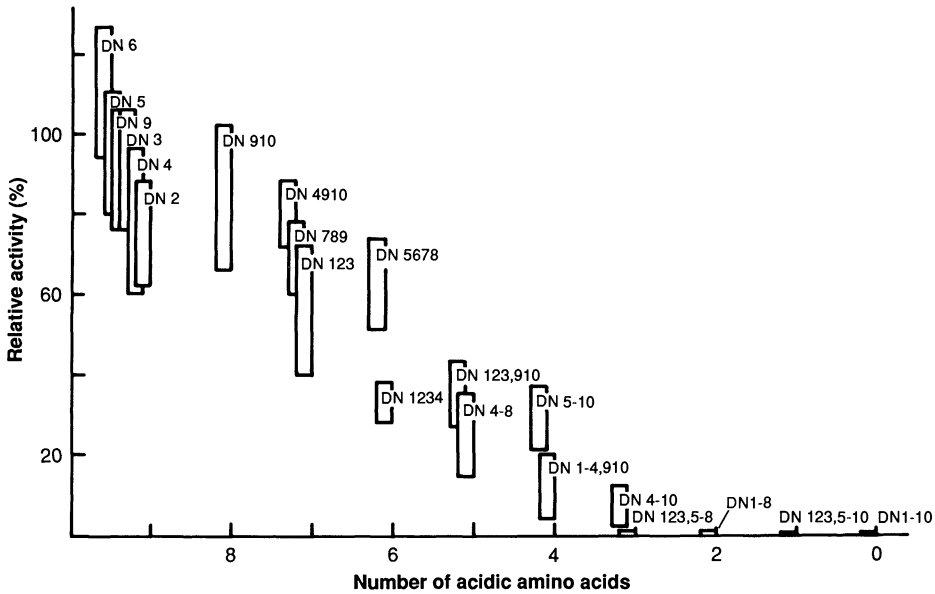

Fig. 2. Relation between net negative charge and relative activities of VP16 derivatives. The relative activities of 21 VP16 derivatives are plotted as a function of remaining acidic amino acids. The derivative designations indicate the amino acid substitutions made (DN: Asp to Asn; for simplicity this nomenclature ignores the fact that acidic amino acid 2 is glutamate) and the acidic amino acid positions affected (number 1 through 10; see Fig. 1). Bars represent two standard deviations about the mean activities determined from at least six transient expression assays (*3*). Mouse L cells (10^6 cells per 60-mm culture plate) were transfected with an indicator plasmid (2 μg of pICP4-*tk*) that contained IE gene regulatory sequences fused to the body of the HSV-1 *tk* reporter gene, an internal control plasmid (2 μg of pMSV-*tk*; *18*), and an activating plasmid (50 ng) that expresses the VP16 del456 polypeptide or a derivative thereof. The ICP4-*tk* and MSV-*tk* RNAs yielded primer extension products of 81 and 55 nucleotides, respectively, which were separated by electrophoresis, detected by autoradiography, and quantitated by scintillation spectroscopy. The relative activities of pMSVP16 del456 derivatives were calculated as the ratio of indicator signal to internal control signal, normalized to pMSVP16 del456. Immunoblot analysis with antiserum directed against VP16 (*3*) revealed that all derivative proteins were stably expressed at similar concentrations (*9*).

not disrupt the overall structure of the VP16 polypeptide, for in an assay that tests the ability of VP16 derivatives to interfere with activation by the wild-type protein (*3*), the FP442 derivative protein retained a dominant negative phenotype (*9*).

To determine whether the effect of the proline substitution of Phe^{442} was due to local disruption of helical structure or to the elimination of a critical side group, we replaced Phe^{442} with three helix-compatible amino acids, serine (FS442), alanine (FA442), and tyrosine (FY442). Of these substitutions only tyrosine was able to functionally replace Phe^{442}, producing an activation domain with about one-third the wild-type activity (Fig. 4A). In contrast, substitution of Phe^{442} with the nonaromatic residues alanine and serine completely inactivated VP16. These results demonstrate that the side group of amino acid 442 participates in transcriptional activation by VP16. We suggest that Phe^{442} (and probably other hydrophobic residues) is involved in a hydrophobic interaction either in self-folding or in direct contact with the molecular target of VP16.

The environment around Phe^{442} may also be important for activation. The VP16 mutant DN5678, in which the four aspartate residues closest to Phe^{442} (Fig. 1) have been replaced by asparagine, is relatively active (62 ± 11%). To study the effects of making less conservative changes in the vicinity of Phe^{442}, we changed the four proximal aspartate residues to glutamate (DE5678) or alanine (DA5678). Glutamate, even though it conserves negative charge, was a slightly poorer replacement (40 ± 10%) than asparagine (Fig. 4B), suggesting that glutamate may slightly disrupt an important structural element conserved by asparagine. Finally, alanine, which conserves neither charge nor side chain structure, was a very poor substitute for aspartate (15 ± 5%). We conclude that the side chain structures of amino acids that flank Phe^{442} are important for transcriptional activation.

In an effort to identify features common to various transcriptional activators and consistent with the results presented here, we aligned the amino acid sequences of three recognized classes of activation domains (*10*) using as a guide the six bulky hydrophobic residues of the minimal activation region of VP16 (Fig. 5). Remarkably, the acidic activation domain of VP16 is most similar to the glutamine-rich transcriptional activation domains of Sp1 (*11*); all six bulky hydrophobic residues of VP16 can be aligned with bulky hydrophobic residues of Sp1, and eight of the ten VP16 acidic amino acids can be directly aligned with glutamine residues in the Sp1 domain A. Uncharged, carbonyl-containing residues can functionally replace aspartate residues in the VP16 activation domain, with some decrease in transcriptional activation (Fig. 4B). The Sp1 activation domains may be uncharged (and thus less active) analogs of the stronger VP16 activation domain, which nonetheless utilize similar hydrophobic contacts. The similarities between VP16 and other acidic or proline-rich activators (Fig. 5) are not as striking as for Sp1. However, each of these proteins contains a motif characterized by a preponderance of carbonyl-containing amino acids that flank bulky hydrophobic residues, similar to the sequence surrounding the critical phenylalanine of VP16.

Our results imply that both ionic and structure-specific hydrophobic interactions are critical to the function of the VP16 activation domain. We predict that VP16 initially finds its molecular target or targets through long-range electrostatic attraction. After the ionic attraction has pulled VP16 and its target or targets into close proximity, van der Waals interactions might predominate to allow intimate binding and perhaps conformational changes necessary to stimulate transcription. The nature of the molecular target for VP16 and other transcriptional activators is currently the subject of intense interest. Several recent reports implicate factors, termed coactivators or adaptors, that may couple activation domains to the transcriptional machinery (*12*). An alterna-

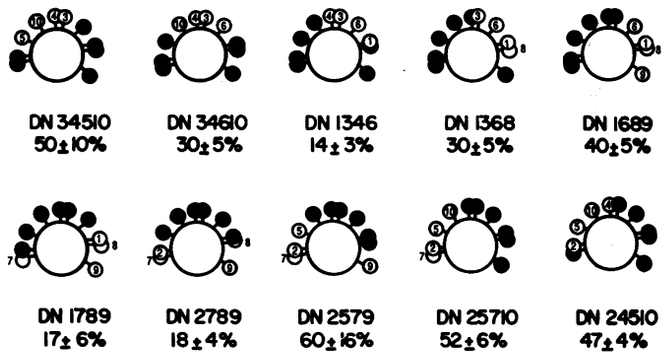

Fig. 3. The VP16 activation domain does not activate transcription as a function of its predicted amphipathy. In the schematic helical wheel models that represent the predicted structure of ten VP16 derivatives, filled circles represent wild-type acidic amino acids and numbered circles represent altered sites. The relative activity (mean ± standard deviation) of each derivative was determined as described in legend to Fig. 2.

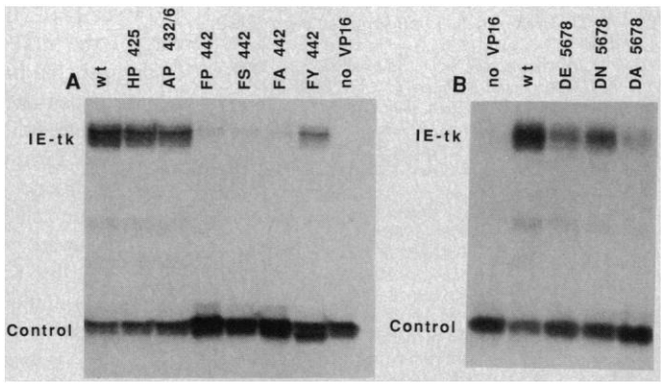

Fig. 4. VP16 Phe^{442} and proximal amino acids are critical in transcriptional activation. (**A**) Autoradiogram of a transient expression assay (performed as in Fig. 2) of several VP16 derivatives designed to test the role of predicted helicity in VP16 activation. The positions of primer extension products corresponding to transcripts from the reporter (IE-*tk*) and control plasmids are indicated. (**B**) Autoradiogram of a transient expression assay of three VP16 derivatives designed to test the importance of the local environment of Phe^{442}.

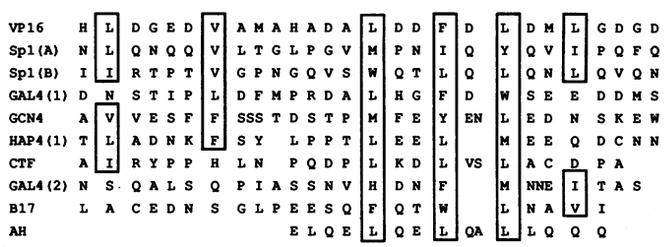

Fig. 5. The amino acid sequences (*16*) of the activation domains of three recognized classes of transcriptional activators (*10*) are aligned using the six bulky hydrophobic residues (boxed) of the VP16 activation domain. Alignments are based upon visual inspection aided by sequence comparison programs (*19*), but do not necessarily represent the most parsimonious alignment. Sp1 (*11*) and CCAAT transcription factor (CTF) (*20*) are mammalian transcriptional activators of the glutamine-rich and proline-rich classes, respectively. GAL4, GCN4, and HAP4 are yeast acidic transcriptional activator proteins (*7*). B17 (*21*) and AH (*8*) are an *Escherichia coli* DNA fragment and an artificial sequence, respectively, which when fused to sequences encoding the GAL4 DNA-binding domain activate transcription in yeast.

tive and not necessarily inconsistent model suggests that a molecular target is the TATA-binding factor TFIID (*13*). The VP16 activation domain selectively and directly binds yeast and human TFIID polypeptides in vitro (*14*). Furthermore, the affinity of in vitro binding of TFIID by various VP16 derivatives (*15*) correlates with the activity of the VP16 activation domain in vivo. These results strongly suggest that the mechanism of activation by VP16 involves a direct interaction with TFIID.

REFERENCES AND NOTES

1. L. E. Post *et al.*, *Cell* **24**, 555 (1981); M. E. M. Campbell *et al.*, *J. Mol. Biol.* **180**, 1 (1984).
2. T. M. Kristie and B. Roizman, *Proc. Natl. Acad. Sci. U.S.A.* **84**, 71 (1987); S. J. Triezenberg, K. L. LaMarco, S. L. McKnight, *Genes Dev.* **2**, 730 (1988); T. Gerster and R. G. Roeder, *Proc. Natl. Acad. Sci. U.S.A.* **85**, 6347 (1988); C. M. Preston *et al.*, *Cell* **52**, 425 (1988); P. O'Hare and C. R. Goding, *ibid.*, p. 435; C. I. Ace, M. A. Dalrymple, F. H. Ramsay, V. G. Preston, C. M. Preston, *J. Gen. Virol.* **69**, 2595 (1988); G. Werstuck and J. P. Capone, *Gene* **75**, 213 (1989); *J. Virol.* **63**, 5509 (1989); R. F. Greaves and P. O'Hare, *ibid.* **64**, 2716 (1990).
3. S. J. Triezenberg, R. C. Kingsbury, S. L. McKnight, *Genes Dev.* **2**, 718 (1988).
4. R. Greaves and P. O'Hare, *J. Virol.* **63**, 1641 (1989).
5. I. Sadowski *et al.*, *Nature* **335**, 563 (1988).
6. D. J. Cousens, R. Greaves, C. R. Goding, P. O'Hare, *EMBO J.* **8**, 2337 (1989).
7. I. A. Hope and K. Struhl, *Cell* **46**, 885 (1986); J. Ma and M. Ptashne, *ibid.* **48**, 847 (1987); S. L. Forsburg and L. Guarente, *Genes Dev.* **3**, 1166 (1989); P. J. Godowski, D. Picard, K. R. Yamamoto, *Science* **241**, 812 (1988).
8. E. Giniger and M. Ptashne, *Nature* **330**, 670 (1987); M. Ptashne, *ibid.* **335**, 683 (1988).
9. W. D. Cress and S. J. Triezenberg, unpublished data.
10. P. J. Mitchell and R. Tjian, *Science* **245**, 371 (1989).
11. A. J. Courey and R. Tjian, *Cell* **55**, 887 (1988).
12. B. F. Pugh and R. Tjian, *ibid.* **61**, 1187 (1990); S. L. Berger, W. D. Cress, A. Cress, S. J. Triezenberg, L. Guarente, *ibid.*, p. 1199; R. J. Kelleher *et al.*, *ibid.*, p. 1209; F. Liu and M. R. Green, *ibid.*, p. 1217.
13. M. Horikoshi, M. F. Carey, H. Kakidani, R. G. Roeder, *ibid.* **54**, 665 (1988); M. Horikoshi, T. Hai, Y.-S. Lin, M. R. Green, R. G. Roeder, *ibid.*, p. 1033; T. Hai *et al.*, *ibid.*, p. 1043.
14. K. F. Stringer *et al.*, *Nature* **345**, 783 (1990).
15. C. J. Ingles, M. Shales, W. D. Cress, S. J. Triezenberg, J. Greenblatt, in preparation.
16. Single letter abbrevations for the amino acids are A, Ala; C, Cys; D, Asp; E, Glu; F, Phe; G, Gly; H, His; I, Ile; K, Lys; L, Leu; M, Met; N, Asn; P, Pro; Q, Gln; R, Arg; S, Ser; T, Thr; V, Val; W, Trp; and Y, Tyr.
17. M. J. Zoller and M. Smith, *Nucleic Acids Res.* **10**, 6487 (1982); T. A. Kunkel, *Proc. Natl. Acad. Sci. U.S.A.* **82**, 488 (1985).
18. B. J. Graves, R. N. Eisenman, S. L. McKnight, *Mol. Cell. Biol.* **5**, 1948 (1985).
19. J. Devereux, P. Haeberli, O. Smithies, *Nucleic Acids Res.* **12**, 387 (1984).
20. N. Mermod *et al.*, *Cell* **58**, 741 (1989).
21. J. Ma and M. Ptashne, *ibid.* **51**, 113 (1987).

22. We thank A. Cress, J. Regier, and R. Pichyangkura for thoughtful suggestions and enthusiastic assistance and C. J. Ingles, S. L. Berger, S. L. McKnight, Z. Burton, and L. Kroos for helpful discussions and for critically reading the manuscript. Supported by funds from Michigan State University, the Michigan Agricultural Experiment Station, NIH grant AI 27323, and a Barnett Rosenberg Graduate Fellowship (W.D.C.).

23 July 1990; accepted 1 November 1990

Three-Dimensional Structures of Acidic and Basic Fibroblast Growth Factors

X. ZHU, H. KOMIYA, A. CHIRINO, S. FAHAM, G. M. FOX, T. ARAKAWA, B. T. HSU, D. C. REES*

Members of the fibroblast growth factor (FGF) family of proteins stimulate the proliferation and differentiation of a variety of cell types through receptor-mediated pathways. The three-dimensional structures of two members of this family, bovine acidic FGF and human basic FGF, have been crystallographically determined. These structures contain 12 antiparallel β strands organized into a folding pattern with approximate threefold internal symmetry. Topologically equivalent folds have been previously observed for soybean trypsin inhibitor and interleukins-1β and -1α. The locations of sequences implicated in receptor and heparin binding by FGF are presented. These sites include β-sheet strand 10, which is adjacent to the site of an extended sequence insertion in several oncogene proteins of the FGF family, and which shows sequence conservation among the FGF family and interleukin-1β.

FIBROBLAST GROWTH FACTORS (FGFs) are members of a protein family that induce mitogenic, chemotactic, and angiogenic activity in a variety of cells of epithelial, mesenchymal, and neural origins (*1*). As a consequence of their strong affinity for heparin, FGFs are also referred to as heparin-binding growth factors (HBGFs). Interests in FGFs have centered on the molecular details of the receptor-mediated pathways by which their diverse physiological activities are expressed and the design of therapeutically useful agents that could either mimic or inhibit the action of these growth factors. Acidic FGF (aFGF) and basic FGF (bFGF), two original members of the FGF family, have similar but distinguishable biological activities and exhibit approximately 55% sequence identity (*2, 3*). Five other members of the FGF family have been presently identified on the basis of sequence homology and the ability to modulate cell proliferation and differentiation: four are putative oncogene products [int-2 (*4*), hst/KS3 (*5*), FGF-5 (*6*), and FGF-6 (*7*)], and the fifth is keratinocyte growth factor (*8*). A three-dimensional model for a member of the FGF family would provide a structural framework for discussing the relation between these different proteins and for identifying the spatial locations of residues involved in receptor and heparin binding. In this report we describe the crystallographic structures for both aFGF and bFGF. Strikingly, the FGF family exhibits a folding pattern similar to that observed for the cytokines interleukins-1α and -1β (IL-1α and IL-1β).

X. Zhu, H. Komiya, A. Chirino, S. Faham, B. T. Hsu, D. C. Rees, Division of Chemistry and Chemical Engineering, California Institute of Technology, Pasadena, CA 91125.
G. M. Fox and T. Arakawa, Amgen, Thousand Oaks, CA 91320.

*To whom correspondence should be addressed.

A recombinant analog of bovine aFGF (*9*), in which Cys^{47} and His^{93} were changed to Ala and Gly, respectively, was used in this study. The biological activity of this analogue is equal to or greater than the corresponding natural sequence molecule either with or without heparin. Crystals were grown by vapor diffusion against 0.2 M $(NH_4)_2SO_4$, 2 M NaCl, 0.099 M sodium citrate, and 0.02 M sodium potassium phosphate, pH 5.6. The protein droplet contained equal volumes of the reservoir solution and a 10 mg/ml protein solution. The crystals are trigonal (space group $P3_121$, a = 78.6 Å and c = 115.9 Å) and diffract to 2.5 Å resolution. Intensity data were collected with a Siemens multiwire area detector mounted on an 18-kW rotating-anode generator. The XENGEN (*10*) and ROCKS (*11*) crystallographic packages were used for data reduction and processing. Multiple isomorphous replacement (MIR) phases were calculated to 3 Å resolution from two derivatives, ethylmercurithiosalicylate (EMTS) and K_2PtCl_4, with a figure of merit of 0.68 (Table 1). After solvent flattening (*12*), regions corresponding to two independent aFGF molecules in the asymmetric unit were identified. The general noncrystallographic symmetry relations between these molecules were determined from rotation function, real-space translation function, and density correlation studies (*13–15*). A molecular envelope was defined around an averaged aFGF molecule by a modification of the Wang algorithm (*12*). Phases were then iteratively refined by molecular averaging and solvent flattening (*14*). Initial maps revealed extended regions of β-sheet structure that were truncated at the loops because the molecular envelope was too small. The final map for model building was calculated with MIR phases [from heavy-atom parameters rerefined against averaged phases, as described in (*16*)] and iteratively averaged